VIEWPOINT SELECTION BY PAINTING

Takashi Michikawa, Hiromasa Suzuki
RCAST, The University of Tokyo, Meguro, Tokyo, Japan

Ken-ichi Anjyo
OLM Digital, Setagaya, Tokyo, Japan

Keywords: Viewpoint selection, Painting, Depth buffer.

Abstract: Complex 3D models are very time-consuming to render, and it is difficult to achieve the desired viewpoint for them using interactive methods such as virtual trackballs. This paper presents an intuitive method for computing good camera positions through a simple painting interface. Given a 3D scene, the user simply paints the region of interest (ROI) on the 2D screen, and the camera is repositioned to pan in on it. Since the computation uses depth buffers, it is independent of the complexity of the model; this makes it efficient for viewing complicated 3D models. Here, we also demonstrate several applications in 3D painting, sketching and light placement.

1 INTRODUCTION

Manipulating 3D models to the desired position is a fundamental task in computer graphics, computer-aided design and other related fields. However, it is hard to apply direct 3D operations such as painting and sketching to models in their initial position. Accordingly, the user controls the camera position using a virtual trackball (VT) (Chen et al., 1988; Shoemake, 1992) to pan in on the desired region. In this study, we focus on view navigation techniques for massive 3D models.

Our motivation comes from the visualization and manipulation of massive scanned models. Recent progress in scanning technology enables us to obtain point sets with high resolution, and various communities now utilize scanned data for the preservation of cultural assets and in digital engineering. In these applications, massive point sets are obtained from surface scanners and converted to polygonal models by surface reconstruction algorithms. The size of such polygonal models easily exceeds ten million triangles.

A number of issues related to virtual trackballs come to light when we combine them with massive models. Suppose ten million triangles are examined using a virtual trackball; there are gaps between the user's action and the display results because this is an interactive process and the object must be rendered for each frame. Massive models cannot maintain an efficient FPS rate even if a high-end GPU is used. Although this problem is preventable by using low-resolution models, the user needs to perform many operations to reach the desired point, because a virtual trackball provides only rotation operation, and is independent of translation and scaling.

We present a geometry-driven camera placement technique that uses a painting interface. The method simply involves the user painting the region of interest (ROI). An algorithm then reconstructs the camera position based on this region to pan in on it. Technically speaking, the technique estimates ray direction as a normal vector of the ROI and reconstructs the camera position so that the view volume covers the region.

One of the key points of our method is computation using depth buffers of 2D images. The technique requires mask images of the ROI and the depth buffer of the scene. This provides various benefits as follows:

- It is independent of model complexity.
- Various geometric types are handled.
- The power of graphics APIs can be leveraged.

A painting-based interface also provides a more global and precise way to specify the ROI than conventional GUIs. If an area is specified by picking individual elements, too many faces or vertices must be

Michikawa T., Suzuki H. and Anjyo K..
VIEWPOINT SELECTION BY PAINTING.
DOI: 10.5220/0003360802960301
In *Proceedings of the International Conference on Computer Graphics Theory and Applications* (GRAPP-2011), pages 296-301
ISBN: 978-989-8425-45-4

selected to define the ROI. On the other hand, if it is specified by drawing a rectangle, unnecessary regions are also selected, which affects the results. A painting interface resolves these problems; by painting, the user can select many elements at once and choose only the desired region.

Moreover, our method can be used not only for camera placement but also for other purposes. In this work, we additionally present a number of applications to 3D painting/sketching and decal and light placement.

2 RELATED WORK

2.1 Viewpoint Selection

Ways of achieving the desired camera position have been studied for model recognition and creating thumbnails. Most such methods are based on solving minimization or maximization problems. (Kamada and Kawai, 1988) first studied this issue by minimizing the number of degenerated faces under orthogonal projections. (Lee et al., 2005) maximizes view saliency, or feature points, while (Podolak et al., 2006) maximizes as many symmetry features as possible. (Fu et al., 2008) proposed a method for finding a stable from symmetry and supporting planes by convex hull. (Bordoloi and Shen, 2005; Takahashi et al., 2005) proposed methods for finding viewpoints for volumetric models. These methods involve automatic operations, but only compute viewpoints so that the whole object is fitted into the window; they cannot focus on parts of objects without user interaction.

2.2 Directable Viewpoint Selection

The use of haptic devices provides an intuitive way to manipulate objects. For instance, the *ArtNova* system(Foskey et al., 2002) introduces a viewpoint navigation system similar to that of our approach, in that it allows the user to select the desired point. However, this method allows only a single point to be chosen; our system is more general, and does not require special devices.

The HoverCam(Khan et al., 2005) provides a method for interactive navigation with proxy(simple) objects so that surfaces come to the front of the viewpoint. In addition, multiscale navigation is also enabled by managing proxies by hierarchical data structure. However, this assumes original or proxy surfaces are relatively smooth or it is weak with noisy models. More recently, (McCrae et al., 2009) extended this to image-based methods which enable not

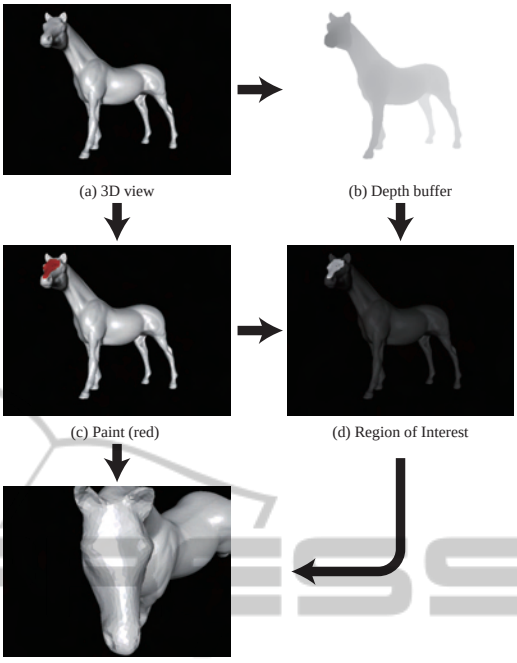

Figure 1: An overview of our algorithm.

only view navigation but also collision detection on GPUs and achieved multi-scale navigation of very large scenes. These methods are also close to ours, however their purpose is different. Our method is designed for viewing and manipulating unstructured massive scanned models with low FPS.

(Hachet et al., 2008) proposed an excellent interface to select viewpoints. Given a point or circle strokes as a region by the users, it gives a 3D widget in the region to control an optimal view. However, this is difficult to find an optimal viewpoint from current view. Although they provide a preview window to help it, they need to render scenes and it may take time for massive models.

3 ALGORITHM

The our method interface is quite simple; users simply paint the region they want to see. Fig. 1 shows an overview of the algorithm used.

Given a 3D scene (a), the depth buffer (b) is first captured from the scene. The results of the painting are stored as a mask image (c), and the depth buffer is then clipped using this image (d). The region of interest or point set $\mathbf{P} = \{\mathbf{p}_i\}$ is computed by the clipped depth buffer. Our algorithm computes camera information C from $\mathbf{P}$ and the current camera information $\hat{C}$(e). According to (Blinn, 1988), C includes follow-

ing components (Fig. 2):

- **e** : eye position
- **c** : center of interest
- **u** : up vector
- θ : the perspective angle of the camera. In this paper, we assume that remains unchanged.

Here, we introduce the method of computation.

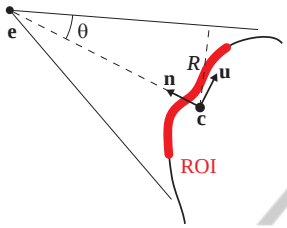

Figure 2: Camera information.

The center of interest is given by taking the weighted center of mass of **P** as shown in Eq.1,

$$\mathbf{c} = \frac{1}{\sum w_i} \sum_{\mathbf{p}_i \in \mathbf{P}} w_i \mathbf{p}_i, \quad (1)$$

where w_i denotes the area around $\mathbf{p}_i$. The reason for introducing w_i is that corresponding points in 3D are sampled non-uniformly.

Next, we ascertain the ray vector **n** for computing **e**. It is natural that **n** is the normal vector of a tangent plane of **P**. Here, we use a method for estimating the normal vector of a point set (Hoppe et al., 1992). We construct a co-variance matrix M of **P** in Eq. 2,

$$M = \sum_{\mathbf{p}_i \in \mathbf{P}} w_i (\mathbf{p}_i - \mathbf{c})^T (\mathbf{p}_i - \mathbf{c}). \quad (2)$$

We use **n** as the eigenvector corresponding to the minimum eigenvalue of M. Then, the direction of **n** satisfies $(\mathbf{n}, \hat{\mathbf{n}}) > 0$, where $\hat{\mathbf{n}}$ denotes the normal vector of the current scene.

The eye point **e** can then be reconstructed from **c** and **n** using Eq. 3,

$$\mathbf{e} = \mathbf{c} + \frac{R}{\sin\theta}\mathbf{n}, \quad (3)$$

where R and θ denote the radius of bounding sphere of **P** and the field of view angle in the current perspective view, respectively (Fig. 2).

By using **n** and $\hat{\mathbf{n}}$, we can obtain a rotation matrix R such that $\mathbf{n} = R\hat{\mathbf{n}}$. The up vector **u** is computed by R using Eq. 4,

$$\mathbf{u} = R\hat{\mathbf{u}}. \quad (4)$$

Finally, the camera position is updated by the graphics API (e.g., **gluLookAt()**).

3.1 Outlier Removal

Our algorithm is weak with irregular points (outliers) (shown in the yellow circle in Fig. 3(c)) caused by mispainting (Fig. 3(a) and (b)) or scanning noises because they affect the covariance matrix in Eq. 2, and invalid ray vectors are computed (Fig. 3(c)). Of course, such points can be removed by erasing the paint, but we introduce an automatic removal method using global optimization solutions such as graph-cut (Boykov and Kolmogorov, 2004).

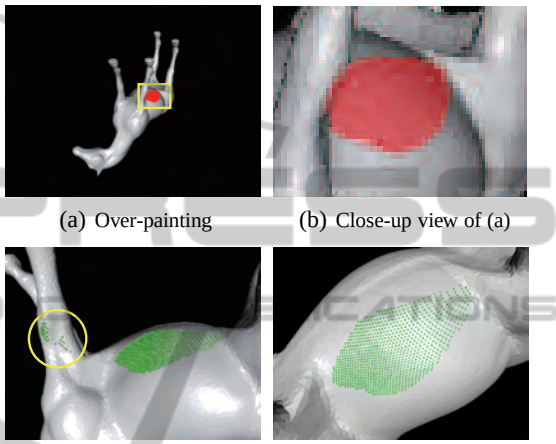

(a) Over-painting (b) Close-up view of (a)

(c) Result w/o graph-cut (d) Result with graph-cut

Figure 3: Outlier removal by graph-cut segmentation. The green spheres are 3D points unprojected from depth buffers.

The graph-cut algorithm is a minimum-cut algorithm for graphs (Fig. 4), and is widely used in image processing problems. We use it to automatically remove outliers caused by mispainting (Fig.3 (c)). However, cost assignment is a difficult task. Here, we discuss a strategy to assign costs between nodes for graph-cut application.

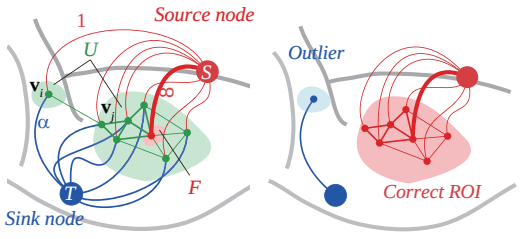

(a) Cost setting (b) Minimum cut

Figure 4: Graph cut segmentation in outlier removal.

From observation of Fig. 3 , we can draw the following assumptions:

1. The mispainted region is relatively small, and creates small clusters (Fig. 4(a)).

2. The depth value of the mispainted region is significantly different from that of the correct region.

From assumption 1, we can extract a point set $F = \{\mathbf{f}_i\}$ that must belong to the correct ROI (Fig. 4 (a)). These can be obtained by taking the k-th nearest points from the median of the depth buffers in P. The other points $U = \{\mathbf{u}_i\}$ are considered as unknown. Now we assign a weight to each edge between $\mathbf{v}_i$ and source/sink nodes as shown in Eq. 5,

$$w(\mathbf{v}_i, S) = \begin{cases} \infty & \mathbf{v}_i \in F \\ 1 & \mathbf{v}_i \in U \end{cases}, \quad w(\mathbf{v}_i, T) = \begin{cases} 0 & \mathbf{v}_i \in F \\ \alpha & \mathbf{v}_i \in U \end{cases}, \tag{5}$$

where S and T are the roots of the source and sink nodes respectively. α is a parameter to control the results.

Next, we assign a weight to each edge between neighboring nodes $\mathbf{v}_i$ and $\mathbf{v}_j$ based on assumption 2. If two nodes are close to each other, they are hard to cut and their cost must be low and vice versa. The cost function between nodes is given by Eq. 6.

$$E(\mathbf{v}_i, \mathbf{v}_j) = \frac{\beta}{||\mathbf{v}_i - \mathbf{v}_j||}, \tag{6}$$

where β is a user-given parameter.

Fig. 3 shows an example. Here, the user intends to paint the body of the horse model. We apply graph-cut in the preprocessing phase to remove such noise before the viewpoint computation phase. It is seen that the expected results can be computed as a result of outlier removal from Figure 3(d). In this case, $\alpha = 10$ and $\beta = \mathrm{diag}(P)$: diagonal length of the bounding box of P used.

4 RESULTS AND DISCUSSION

4.1 Implementation

We implemented a prototype system with OpenGL and GLUT. Note that this algorithm can be implemented without any special functions. For instance, **glReadPixels()** is used to capture depth buffers, and **gluUnproject()** is used to compute 3D points from depth values. This means the algorithm does not require expensive GPUs.

4.2 Results

Figs. 1, 5, 6 and 7 show several results obtained using our method. In each figure, (a) shows the input camera position with the ROI drawn in red, and (b) shows the reconstruction resulting from this technique.

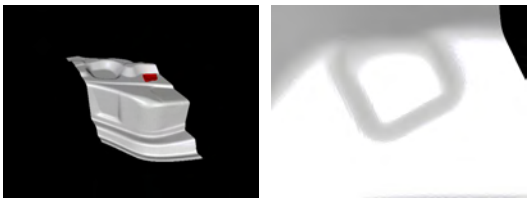

(a) (b)

Figure 5: Results for scanned objects(120,303 triangles).

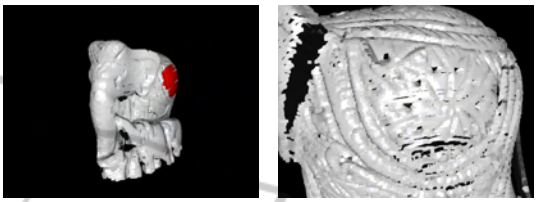

(a) (b)

Figure 6: Results for a scanned point set (1,282,225 points).

4.3 Discussion

Figs. 1, 5, 6 and 7 demonstrate results for point sets and polygons. These figures show that our method can be applied to various types of geometric models. This is because geometry is captured from depth buffers, and intersections between rays and objects are not considered.

Our method retrieves geometry from depth buffers, and does not render during the navigation phase. This means that there are not gaps between user action and display results even with massive models. Fig. 7 shows a model of David with over ten million triangles. With such complex models, it usually takes a long time to reach the desired position. However, our method achieves appropriate position with a single user action.

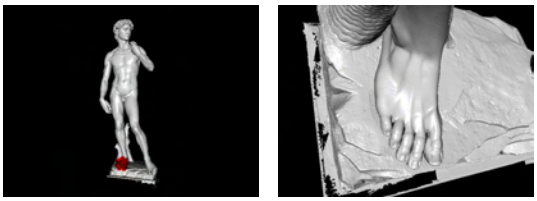

(a) (b)

Figure 7: Results for complex models(11,169,874 triangles).

Fig. 8 shows computational statistics for finding viewpoint described in Section 3. All examples are measured in the following environments :

- 32 bit : Intel Core 2 Duo 2.13GHz + GeForce 7300GS (521MB)

- 64 bit : Intel Xeon 3.16GHz + QuadroFX 1700 (512MB)

Note that the David model cannot be rendered on a 32-bit OS due to memory allocation error. We can see computation time for each example is almost same, although the number of elements is different. On the other hand, the size of the frame buffer affects performance because it takes much time to retrieve the depth buffer.

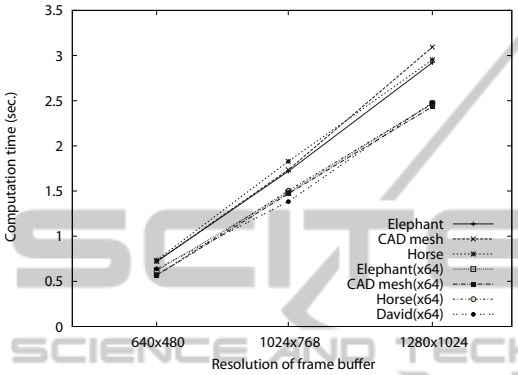

Figure 8: Statistics.

One of advantages of paint-based interface is to specify complex ROIs as shown in Fig. 9. In this example, we paint four soles of the horse model(a), and our method computes the viewpoint so that we can see them at once(b). Note that other methods(rectangle and cursor) cannot work well. This is because they capture unnecessary region, and invalid viewpoint will then be computed.

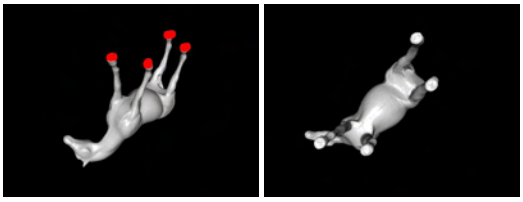

(a) Paint (b) Result

Figure 9: Focus on multiple ROIs.

The quality of C depends on that of the depth buffer. If the near and far clipping planes are far from each other, the precision of the depth value is worse when the surface is close to the far clipping plane[1]. Accordingly, we need to consider clipping plane management to ensure a tight fit to the model. This can be resolved by finding min/max depth values and using them as clipping planes.

[1]http://www.opengl.org/resources/faq/technical/depthbuffer.htm

5 APPLICATIONS

5.1 3D Painting and Sketching

Direct painting and sketching onto 3D surfaces is an intuitive method for the modeling process. Accordingly, it is better for capturing and focusing on surfaces on which users paint or sketch. Fig. 10 shows a framework of 3D painting with our method interface implemented in Autodesk Maya. A good viewpoint for 3D painting can be obtained through this method with a single user action, thus accelerating the painting process.

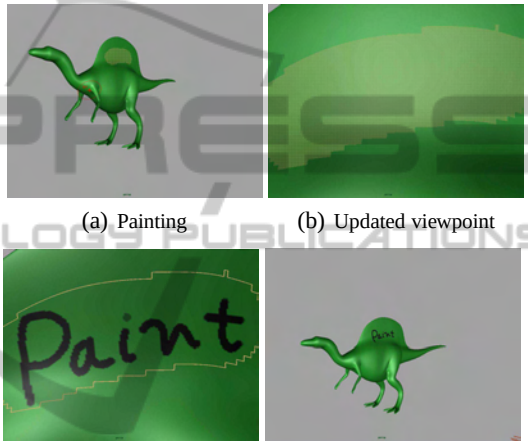

(a) Painting (b) Updated viewpoint

(c) Painting on the surface (d) Result. Back to (a)

Figure 10: Framework of 3D painting with our method.

This technique can be used not only for painting and sketching but also for decal arrangement. Since decal placement uses projection mapping, it is difficult to achieve the desired direction when mapping decals onto curved or bumpy surfaces. Fig. 11 shows an example of decal arrangement in Maya. Here, we map a decal texture (a) onto the left eye of a horse model (b). our method is used to compute the projection plane.

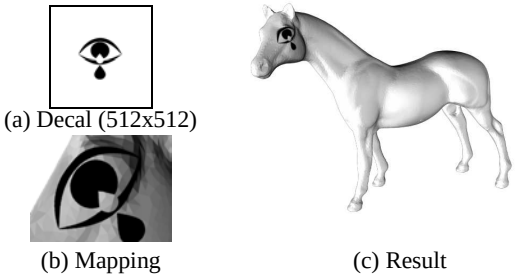

(a) Decal (512x512)

(b) Mapping (c) Result

Figure 11: Example of decal arrangement with our method.

5.2 Light Placement

Our algorithm can also position lights appropriately (Fig. 12). The interface is almost the same as that for camera placement. The user paints the region where the light is needed, and the algorithm creates a spotlight to illuminate the area specified. The light position, the direction and cut-off ratio for the spot light correspond to the **e**, **n** and θ in Section 3 respectively. This is efficient for CG animations. In CG production, there is often a need to place lights in an eccentric position to obtain plausible shading.

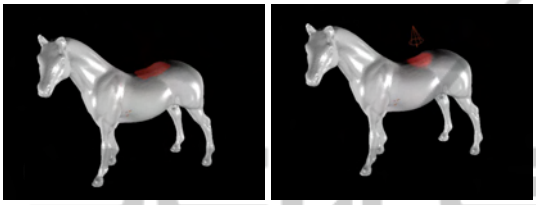

(a) Painting ROI (b) Lighting result

Figure 12: Light placement by painting.

6 CONCLUSIONS

We have presented a painting interface for camera placement. Our algorithm requires only specification of the region of interest by painting, and the camera is then repositioned based on the ROI. We remark that our method is not the alternative of other existing methods, and we suppose to use the proposed method with them. For instance, we use our method for finding intial viewpoint and we adjust the viewpoint by other methods(e.g. zoom out).

We also have plans for related future work. First, the good up vector need to be computed. Second, we would like to extend this method to volumetric models or we would like to find a viewpoint by direct painting on volume rendering display.

ACKNOWLEDGEMENTS

Models are cortesy of Georgia Tech(Fig.1), AIM@shape(Fig. 6) and Stanford Digital Michelangelo Project (Fig. 7). This work is partially suppoted by KAKENHI (No. 22246018, No. 22700091).

REFERENCES

Blinn, J. (1988). Where Am I? What Am I Looking At? *IEEE CG&A*, 8(4):76–81.

Bordoloi, U. D. and Shen, H.-W. (2005). View selection for volume rendering. *IEEE Visualization*, 0:487–494.

Boykov, Y. and Kolmogorov, V. (2004). An experimental comparison of min-cut/max-flow algorithms for energy minimization in vision. *IEEE PAMI*, 26(9):1124–1137.

Chen, M., Mountford, S. J., and Sellen, A. (1988). A study in interactive 3-d rotation using 2-d control devices. In *SIGGRAPH '88*, pages 121–129.

Foskey, M., Otaduy, M. A., and Lin, M. C. (2002). Artnova: Touch-enabled 3d model design. In *IEEE Virtual Reality*, page 119.

Fu, H., Cohen-Or, D., Dror, G., and Sheffer, A. (2008). Upright orientation of man-made objects. *ACM Transactions on Graphics*, 27:42:1–42:7.

Hachet, M., Decle, F., Knödel, S., and Guitton, P. (2008). Navidget for easy 3d camera positioning from 2d inputs. In *Proceedings of IEEE 3DUI*, pages 83–88.

Hoppe, H., DeRose, T., Duchamp, T., McDonald, J., and Stuetzle, W. (1992). Surface reconstruction from unorganized points. In *SIGGRAPH '92*, pages 71–78.

Kamada, T. and Kawai, S. (1988). A simple method for computing general position in displaying three-dimensional objects. *Comput. Vision Graph. Image Process.*, 41(1):43–56.

Khan, A., Komalo, B., Stam, J., Fitzmaurice, G., and Kurtenbach, G. (2005). Hovercam: interactive 3d navigation for proximal object inspection. In *I3D '05*, pages 73–80, New York, NY, USA. ACM.

Lee, C. H., Varshney, A., and Jacobs, D. W. (2005). Mesh saliency. In *ACM SIGGRAPH 2005 Papers*, pages 659–666.

McCrae, J., Mordatch, I., Glueck, M., and Khan, A. (2009). Multiscale 3d navigation. In *I3D '09*, pages 7–14, New York, NY, USA. ACM.

Podolak, J., Shilane, P., Golovinskiy, A., Rusinkiewicz, S., and Funkhouser, T. (2006). A planar-reflective symmetry transform for 3d shapes. In *ACM SIGGRAPH 2006 Papers*, pages 549–559.

Shoemake, K. (1992). Arcball: a user interface for specifying three-dimensional orientation using a mouse. In *Graphics interface '92*, pages 151–156.

Takahashi, S., Fujishiro, I., Takeshima, Y., and Nishita, T. (2005). A feature-driven approach to locating optimal viewpoints for volume visualization. *IEEE Visualization*, 0:495–502.